

Catalysis

How to cite: *Angew. Chem. Int. Ed.* **2020**, *59*, 18709–18716

International Edition: doi.org/10.1002/anie.202008365

German Edition: doi.org/10.1002/ange.202008365

Experimental and Computational Investigations of the Reactions between α,β -Unsaturated Lactones and 1,3-Dienes by Cooperative Lewis Acid/Brønsted Acid Catalysis

Anja Weber, Martin Breugst,* and Jörg Pietruszka*

Abstract: The reactions of α,β -unsaturated δ -lactones with activated dienes such as 1,3-dimethoxy-1-[(trimethylsilyl)oxy]-1,3-butadiene (Brassard's diene) are barely known in literature and show high potential for the synthesis of isocoumarin moieties. An in-depth investigation of this reaction proved a stepwise mechanism via the vinylogous Michael-products. Subsequent cyclisation and oxidation by LHMDS and DDQ, respectively, provided six mellein derivatives (30–84%) and four angelicoin derivatives (40–78%) over three steps. DFT-calculations provide insights into the reaction mechanism and support the theory of a stepwise reaction.

Introduction

Isocoumarins **1–6**, δ -valerolactones with a fused 1,3-dihydroxybenzene, are prominent structural moieties in natural products. One example containing an isocoumarin moiety, is the marine natural product psymberin (**2**), also named irciniastatin A (**2**) (Figure 1).^[1–9] They were isolated independently from marine sponges *Psammocinia* sp. and *Ircinia ramosa* by the two groups of Crews^[7] and Pettit in 2004.^[8] The structures were elucidated and claimed to be diastereoisomers, which was revised later by the first total synthesis and stereochemical assignment by de Barbander and co-workers.^[3] Psymberin (**2**) has been tested on 60 different human cancer cell lines according to the NCI developmental therapeutics in vitro screening program. It showed promising cytotoxicity against melanoma, breast, and

colon cancer cell lines ($LC_{50} < 2.5 \times 10^{-9}$ M).^[7] Cladosporin (**3**) is another mentionable natural product, which was first isolated from fungi *Cladosporium cladosporioides* by van Waalbeek and co-workers in 1971 (Figure 1).^[10] The first asymmetric total synthesis was published by the group of She.^[11] Compound **3** shows promising antimalarial activity.^[12,13]

Mellein (**4a**) is one of the simplest isocoumarin containing natural products.^[14] Mellein (**4a**) and its derivatives have shown a wide biological activity range from antibacterial, antifungal to HCV-protease inhibitory effects.^[15–18] The (*S*)-configured enantiomer is named angelicoin B (**4b**).^[19,20] The tricyclic alternariol (**5**) is a mycotoxin, which leads to crop loss.^[21] Alternariol (**5**) and its derivatives show high activity against bacteria, fungi, and cytotoxicity on human cancer cell lines.^[22] The Podlech group synthesised alternariol (**5**) in seven steps from orcinol and 3,5-dimethoxybromobenzene in 2005, probably providing the best access to this compound today.^[23] One of the most recently isolated natural compounds with an isocoumarin moiety is flavoseoside (**6**) from *Malbranchea flavorose*. The structure could be elucidated in 2017.^[24]

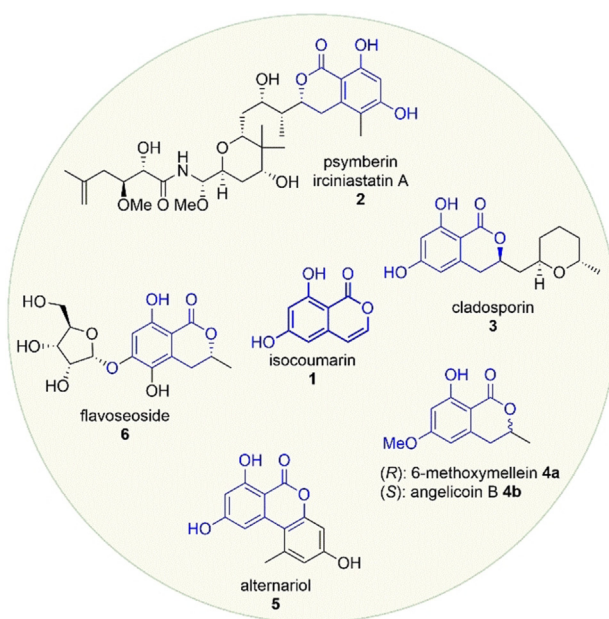


Figure 1. Selected structures of natural products containing an isocoumarin moiety (blue).

[*] Dr. A. Weber, Prof. Dr. J. Pietruszka
Institut für Bioorganische Chemie, Heinrich-Heine-Universität Düsseldorf im Forschungszentrum Jülich
Stettener Forst, Geb. 15.8, 52426 Jülich (Germany)
E-mail: j.pietruszka@fz-juelich.de

Priv.-Doz. Dr. M. Breugst
Department für Chemie, Universität zu Köln
Greinstraße 4, 50939 Köln (Germany)
E-mail: mbreugst@uni-koeln.de

Prof. Dr. J. Pietruszka
Institut für Bio- und Geowissenschaften: Biotechnologie (IBG-1),
Forschungszentrum Jülich GmbH
52428 Jülich (Germany)

Supporting information and the ORCID identification number(s) for the author(s) of this article can be found under:
<https://doi.org/10.1002/anie.202008365>.

© 2020 The Authors. Published by Wiley-VCH GmbH. This is an open access article under the terms of the Creative Commons Attribution License, which permits use, distribution and reproduction in any medium, provided the original work is properly cited.

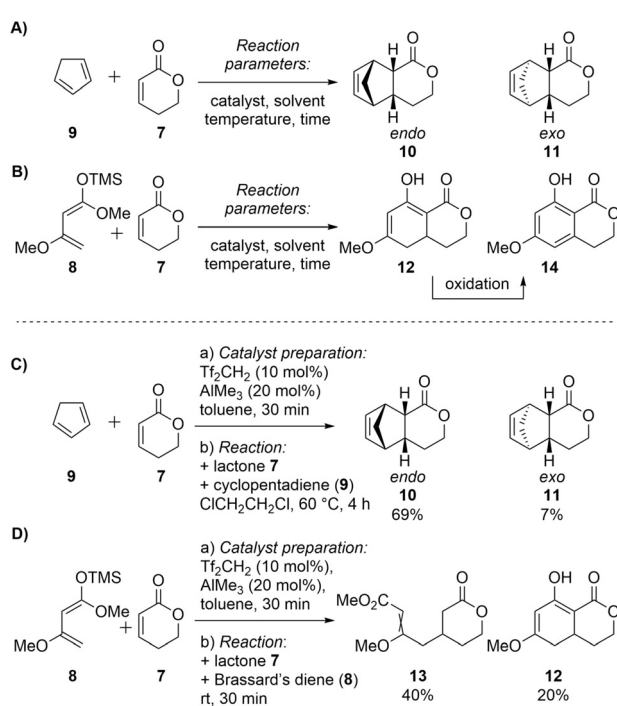
All these examples show that there is a need for a short and efficient synthesis of isocoumarins **1–6** and their derivatives as building blocks for natural product synthesis. For the increasing necessity of new drugs, caused by the growing population, resistances, and new diseases, we need to understand the mode of action of drugs, but also the chemical reactions. Therefore, it is a major challenge to develop general and predictable methods to achieve building block syntheses such as isocoumarins in an applicable way.

Currently, only few methods are established for the reaction of α,β -unsaturated lactones with unsubstituted 1,3-dienes,^[25,26] alkynes,^[27] and bis(SiEt₃)-substituted dienes^[28] towards bicyclic isochromenones, whereupon none leads to 6,8-dihydroisochroman-1-ones. The reported methods describe a concerted Diels–Alder type reaction between α,β -unsaturated δ -lactones with different types of dienes. The Diels–Alder [4+2]-cycloaddition reaction is a powerful tool for the formation of C–C bonds and the synthesis of six-membered rings. Accordingly, it is widely used in natural product synthesis and for industrial application.^[29,30] Here we report a short synthesis of isocoumarins from α,β -unsaturated lactones with 1,3-dienes also providing some theoretical insight into the reaction mechanism. DFT calculations were used to describe the reaction mechanism of 5,6-dihydro-2*H*-pyran-2-one (**7**) with (*Z*)-[(1,3-dimethoxybuta-1,3-dien-1-yl)oxy]trimethylsilane (Brassard's diene **8**).^[31] The combination of experimental and theoretical investigations then allowed us to propose a reaction mechanism for the isocoumarin formation.

Results and Discussion

Initial Screening. Initially, it was anticipated to perform a *Diels–Alder* reaction between an α,β -unsaturated δ -lactone and activated dienes such as Brassard's diene (**8**), thus obtaining isocoumarins as natural product building blocks after oxidation (Scheme 1). The initial reactions were examined with commercially available 5,6-dihydro-2*H*-pyran-2-one (**7**) as a model dienophile and freshly distilled cyclopentadiene (**9**) (Scheme 1A) or freshly prepared Brassard's diene (**8**) (Scheme 1B). The reaction of 5,6-dihydro-2*H*-pyran-2-one (**7**) with cyclopentadiene (**9**), was already known and used as a positive control for the tested reaction parameters.^[26,32,33]

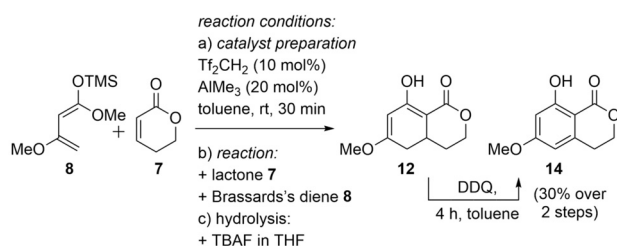
After an extensive catalyst [Lewis acids: AlBr₃, AlMe₃, AlCl₃, Sc(OTf)₃, Yb(OTf)₃, Sm(OTf)₃, ZnCl₂, ZnI₂, ZnBr₂, EtAlCl₂; Brønsted acids: Tf₂CH₂, Tf₂NH], solvent (toluene, dichloromethane, acetonitrile, dichloroethane, *n*-pentane), and temperature screening (–20 °C up to 100 °C), we found that the best working catalyst system was a combined system, using AlMe₃ as Lewis acid and Tf₂CH₂ as Brønsted acid.^[33] Under all tested conditions without catalyst the reaction did not occur. Utilizing cyclopentadiene (**9**) as diene at 60 °C, 69% *endo*-product **10** and 7% *exo*-product **11** were obtained after 4 h when using 20 mol% AlMe₃ and 10 mol% Tf₂CH₂ (Scheme 1, C). The same catalyst loadings also gave the desired 8-hydroxy-6-methoxy-3,4,4a,5-tetrahydro-1*H*-isochroman-1-one (**12**) when 5,6-dihydro-2*H*-pyran-2-one (**7**)



Scheme 1. A) Diels–Alder product of α,β -unsaturated δ -lactone **7** and cyclopentadiene (**9**) as positive control. B) Initial approach towards Diels–Alder product after desilylation and subsequent oxidation. C) Reaction conditions for Diels–Alder reaction between α,β -unsaturated δ -lactone **7** and cyclopentadiene (**9**). D) Reaction conditions for reaction between α,β -unsaturated δ -lactone **7** and Brassard's diene (**8**).

and freshly prepared Brassard's diene (**8**) were used. However, the conditions needed to be adapted because of the low stability of the diene at elevated temperature. Furthermore, low yields of about 10% were observed after one-hour reaction time in dichloroethane at room temperature. TLC and NMR analysis suggested full conversion of α,β -unsaturated δ -lactone **7** and Brassard's diene **8**, but indicated the formation of various side products. Changing the solvent to toluene and decreasing the reaction time to 30 minutes doubled the yield of the product to 20%, but also gave the vinylogous Michael addition product methyl 3-methoxy-4-(2-oxotetrahydro-2*H*-pyran-4-yl)but-2-enoate (**13**) as the major product with 40% yield (Scheme 1D). Later this product was identified as the (*E*)-configured product by nOe experiments.

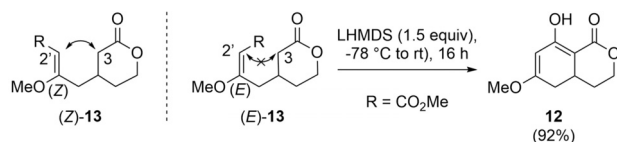
Improving the Sequence. Obviously, the low conversion to diene **12** led to low yields of the desired product **14**. Different catalyst ratios (Tf₂CH₂:AlMe₃ = 1:1, 1:2, 1:3) were tested with 10 mol% Tf₂CH₂ and 20 mol% AlMe₃ showing the best results. Furthermore, it was observed that the workup conditions were strongly influencing the yield. Two main aspects were considered for optimization, a) hydrolysis of the silyl ketene acetal and b) oxidation towards the aromatic product (Scheme 2; for details see Supporting Information). 2,3-Dichloro-5,6-dicyano-1,4-benzoquinone (DDQ) (1.3 equiv, 4 h, quant.) gave the best results providing the desired isocoumarin **14** in quantitative yield from 8-hydroxy-6-methoxy-3,4,4a,5-tetrahydro-1*H*-isochroman-1-one (**12**), and hence we exclusively used DDQ for further oxidations.



Scheme 2. Diels–Alder type reaction of Brassard's diene (**8**) and 5,6-dihydro-2*H*-pyran-2-one (**7**).

Next, various conditions were tested for the hydrolysis of the silyl derivatives leading first to 6-hydroxy-8-methoxy-3,4,4a,5-tetrahydro-1*H*-isochromen-1-one (**12**) and after oxidation to 8-hydroxy-6-methoxy-3,4,4a,5-tetrahydro-1*H*-isochromen-1-one (**14**). Starting from the initial result using tetra-*n*-butylammonium fluoride (TBAF)^[34] in THF and a yield of 20% over two steps, we tested alternative reagents. However, when directly oxidizing the crude mixture with DDQ without isolation of intermediate **12**, this setup proved superior and isochromen-1-one **14** was isolated in moderate 30% yield.

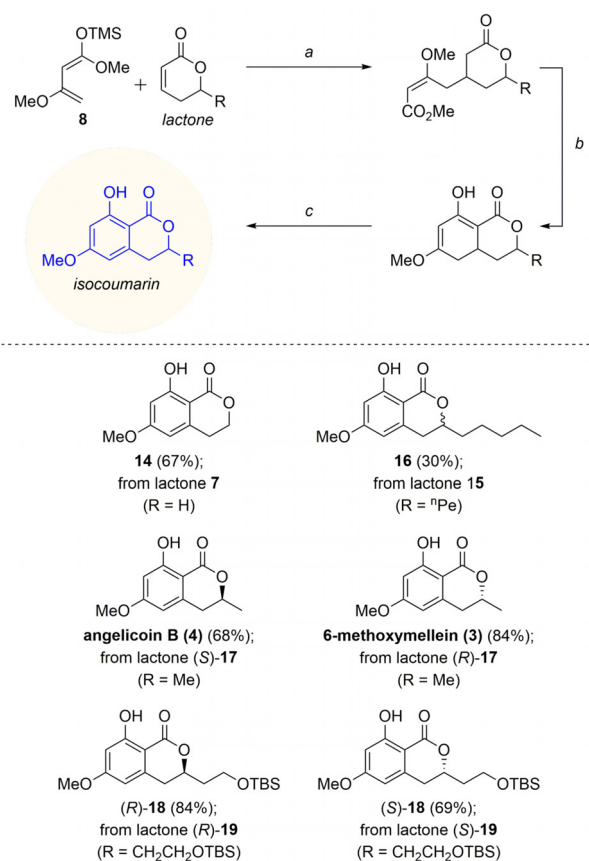
Until now, the yield could be increased from 10% to 30% of the desired 8-hydroxy-6-methoxyisochroman-1-one (**14**), detecting full consumption of the α,β -unsaturated δ -lactone **7** by proton NMR and isolating the vinylogous Michael-product **13** as the major product in 40% yield. Measuring the proton NMR kinetic (see Supporting Information for details) at room temperature in $[\text{D}_8]$ toluene led to the formation of two products. They could be identified after isolation as the presumed vinylogous Michael addition products methyl (*Z*)-3-methoxy-4-(2-oxotetrahydro-2*H*-pyran-4-yl)but-2-enoate [(*Z*)-**13**] and methyl (*E*)-3-methoxy-4-(2-oxotetrahydro-2*H*-pyran-4-yl)but-2-enoate [(*E*)-**13**]. The assignment was based on the observed *n*Oe between 3- H_a and 2'-H for the minor component (*Z*)-**13** (25%) and its absence in the major product (*E*)-**13** (68%, Scheme 3). To conclude, the NMR kinetics showed that the starting materials and intermediates **13** are stable under the reaction conditions, thus establishing a competing vinylogous Michael addition. This was confirmed by the fact that the major isomer [(*E*)-**13**] could be deprotonated at the α -carbon of the lactone, subsequently leading to the desired 6-hydroxy-8-methoxy-3,4,4a,5-tetrahydro-1*H*-isochromen-1-one (**12**) via a Dieckmann condensation. While lithium diisopropylamide (LDA)^[35] gave only low yield, best results (for details see supporting information) were obtained with lithium bis(trimethylsilyl)amide (LHMDS)^[36,37] (92% yield).



Scheme 3. Proton proximity as detected by the *n*Oe coupling between 3- H_a and 2'-H for (*Z*)-**13** (left). Dieckmann reaction vinylogous (*E*)-Michael-product (*E*)-**13** (right).

Substrate scope. After optimization of the catalytic system, the work-up conditions, the Dieckmann reaction as well as the final oxidation, the three-step sequence was combined: The improved protocol led first to a separable mixture of 6-hydroxy-8-methoxy-3,4,4a,5-tetrahydro-1*H*-isochromen-1-one (**12**) (30%) together with (*E*)-**13** (40%). In a consecutive step, the (*E*)-Michael-product (*E*)-**13** could be easily converted to the corresponding 6-hydroxy-8-methoxy-3,4,4a,5-tetrahydro-1*H*-isochromen-1-one (**12**) with LHMDS (92%). Finally, both fractions **12** could be oxidized with DDQ to the desired 8-hydroxy-6-methoxyisochroman-1-one (**14**) in quantitative yield. Over three steps, the isocoumarin **14** was obtained in 67% yield (Scheme 4).

Having established a convenient three-step reaction sequence, the substrate scope was extended to lactones bearing substituents in δ -position. Enantiomerically pure α,β -unsaturated δ -lactones were synthesized via a chemo-enzymatic route,^[38,39] utilizing α -substituted allylboronic esters,^[40,41] or were commercially available. The yields range from 30% ($\text{R} = \text{}^n\text{Pe}$: **15** to **16**) to 84% [$\text{R} = \text{Me}$: (*R*)-**17** to 6-methoxymellein (**3**)]. Besides natural products such as angelicoin B (**4**) [68% from (*S*)-**17**], potential intermediates bearing a common protecting group (TBS: $\text{}^t\text{BuMe}_2\text{Si}$) are also readily available (isocoumarin **18** from the corresponding



a) i) catalyst preparation: Ti_2CH_2 , AlMe_3 , toluene, 30 min, ii) + lactone, + Brassard's diene (**8**), toluene, rt, 10 min; b) $\text{}^n\text{BuLi}$, HMDs, THF, -78°C , ii) THF, -78°C to rt, time; c) DDQ, toluene, 4 h, rt.

Scheme 4. Synthesis of isocoumarins from δ -substituted α,β -unsaturated δ -lactones.

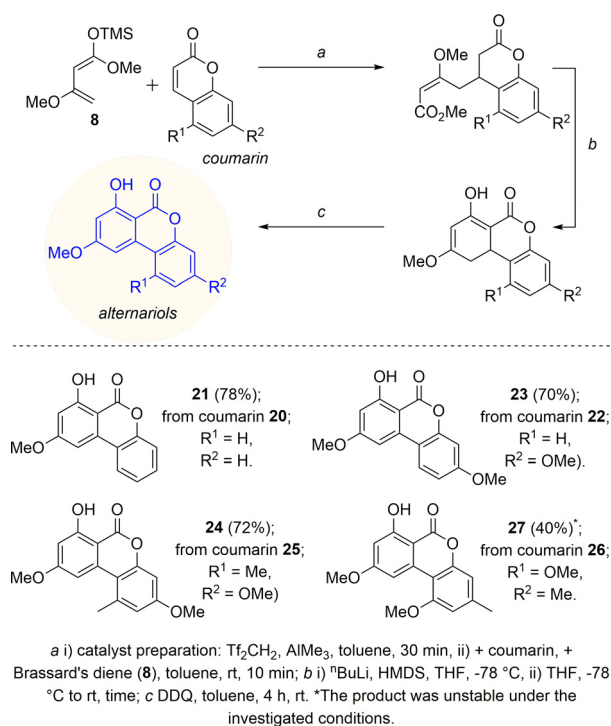
lactone **19**). As expected, no racemization was observed as proven by HPLC analysis of lactone and isocoumarin product.

Next, an expansion of the substrate scope from δ -substituted lactones to coumarins was desirable, generating tricyclic, alternariol-like products. Initially, the reaction with commercially available coumarin **20** (2*H*-chromen-2-one) and Brassard's diene **8** was tested obtaining good yields (78%) of product **21** over three steps (Scheme 5). Unprotected umbelliferon derivatives did not react. However, utilizing 3-methoxy-umbelliferon (**22**)^[42] the reaction worked well (70% of product **23**). 3,9-Dimethoxy alternariol (**24**) could also be synthesized in good yields of 72%. The precursor, 7-methoxy-5-methyl-2*H*-chromen-2-one (**25**), has been synthesized in a Pechmann reaction of 5-methylresorcin with propiolic acid, catalysed by ytterbium(III) trifluoromethanesulfonate^[43] and direct protection of the hydroxyl-group with dimethyl sulfate. The reaction gave the constitutional isomers 5-methoxy-7-methyl-2*H*-chromen-2-one (**26**) and 7-methoxy-5-methyl-2*H*-chromen-2-one (**25**) in a 1:1-ratio. The constitutional isomer 5-methoxy-7-methyl-2*H*-chromen-2-one (**26**) gave the unstable alternariol derivative **27** in moderate yield (40%) over three steps.

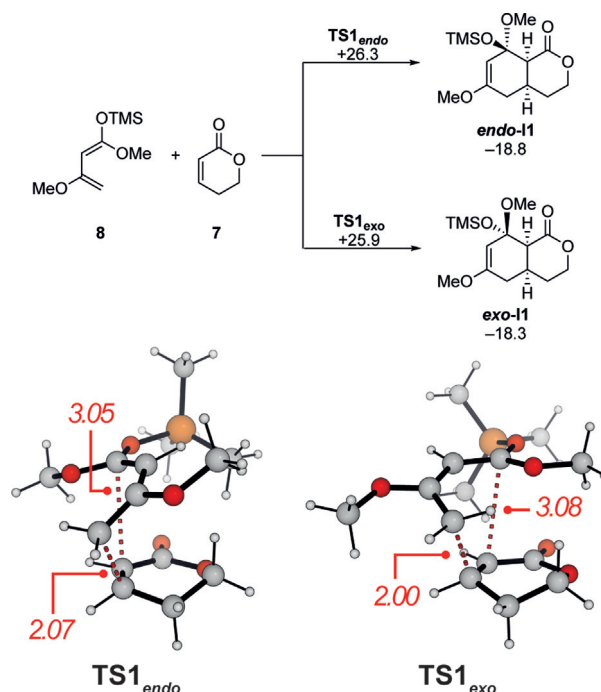
Summary Synthetic Investigation. After extensive catalyst screening, a cooperative catalyst system of AlMe₃ and Tf₂CH₂ was found as the best working system for the investigated reaction. Getting the vinylogous Michael-product as the major product and determining its (*E*)-configuration by nOe measurements, the idea of direct cyclisation of this (*E*)-configured Michael-product towards the desired isocoumarin was established. The crude product could readily be oxidised by DDQ to the desired isocoumarins. Overall, six different

mellein derivatives and four different angelicoin derivatives could be synthesized in moderate to good yields over three steps (30–84%).

Computational investigation. In order to receive more detailed information on the reaction mechanism and to understand as well as explain the unexpected high reactivity of the catalytic system Tf₂CH₂/AlMe₃ in the reactions between α,β -unsaturated lactones and 1,3-dienes, next we carefully analysed the reaction between lactone **7** and Brassard's diene (**8**) computationally [M06-2X-D3/def2-QZVP/IEFPCM(toluene)//M06-L-D3/6-31 + G(d,p)/IEFPCM(toluene)].^[44] In the absence of any catalyst, the reaction between **7** and **8** is thermodynamically favourable to yield *endo*- and *exo*-**11** ($\Delta G = -18.8$ and -18.3 kcal mol⁻¹). The cycloaddition proceeds through transition states **TS1**_{endo} and **TS1**_{exo} of very similar energies ($\Delta G^\ddagger = 26.3$ and 25.9 kcal mol⁻¹). The forming C–C bond lengths significantly differ (2.07 and 2.00 vs. 3.05 and 3.08 Å, Scheme 6) within **TS1** but no zwitterionic intermediates could be identified when following the intrinsic reaction coordinate (IRC) path. In line with this, most zwitterionic structures collapsed to the cycloadducts in separate calculations and stable structures were found to be significantly higher in energy (> 33 kcal mol⁻¹). Therefore, it can be concluded that a putative background reaction should proceed through a concerted, yet asynchronous reaction. The high barrier of ca. 26 kcal mol⁻¹ is qualitatively in line with the experimental finding that no cycloaddition product could be detected even upon heating to 100 °C. Instead, a decomposition of Brassard's diene (**8**) was observed at elevated temperatures.

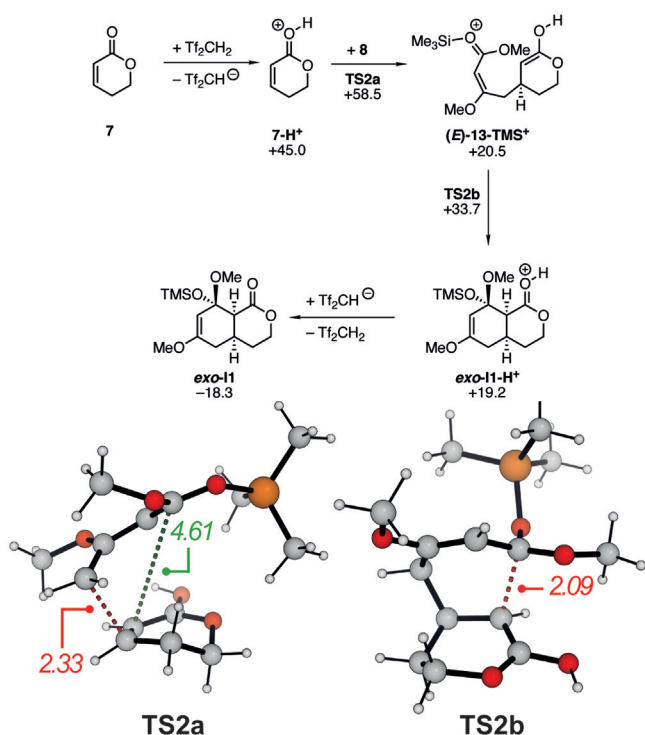


Scheme 5. Synthesis of alternariol derivatives from coumarins.



Scheme 6. Calculated Gibbs free energies (in kcal mol⁻¹) for the uncatalyzed cycloaddition between **7** and **8** (above) and structure as well as selected bond lengths (in Å) for the transition states **TS1** (below).

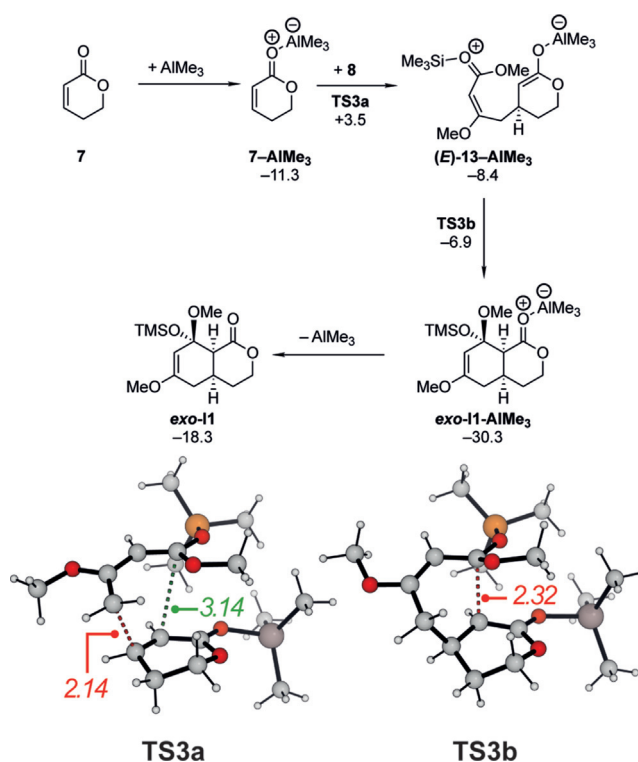
Different mechanistic proposals can be suggested for the $\text{Tf}_2\text{CH}_2/\text{AlMe}_3$ -catalyzed reaction: Brønsted acid catalysis by Tf_2CH_2 or a more acidic $\text{Tf}_2\text{CH}_2\text{-AlMe}_3$ adduct, Lewis acid catalysis by AlMe_3 , or alternative catalytic species formed in the reaction must be considered. We first investigated a Brønsted acid catalysis pathway as summarized in Scheme 7, with selected structures shown. This reaction starts with the protonation of the lactone by Tf_2CH_2 (values for other Brønsted acids like TfOH or HCl are shown in the Supporting Information. According to our calculations, this process is highly endergonic ($+45 \text{ kcal mol}^{-1}$). The value is probably overestimated due to the unfavourable charge separation in the calculations and additional specific solvent-solute interactions not taken into account in continuum models. All attempts to locate concerted pathways failed in these cases and all transition-state guesses resulted in stepwise mechanisms with the formation of a zwitterionic intermediate. The most M06-2X-D3/def2-QZVP/IEFPCM(toluene)//M06-L- transition state for the Brønsted acid catalysis **TS2a** requires an activation free energy of $58.5 \text{ kcal mol}^{-1}$ and results in the unstable zwitterion **(E)-13-TMS⁺**. In this transition state, the length of the forming C–C bond is 2.33 \AA , while the second set of carbon atoms is still well separated (4.61 \AA). Interestingly, transition states leading to a Z-configured double bond within **13-TMS⁺** are significantly lower in energy ($\Delta G^\ddagger = +46.1 \text{ kcal mol}^{-1}$, not shown in Scheme 7). However, these structures are unproductive as they cannot react further to yield the cycloadduct, as observed



Scheme 7. Calculated Gibbs free energies (in kcal mol^{-1}) for the Brønsted acid catalyzed cycloaddition between **7** and **8** (above) and structure as well as selected bond lengths (in \AA) for the transition states **TS2** (below).

and described experimentally. The zwitterion **(E)-13-TMS⁺** then collapses via a small barrier (**TS2b**, $\Delta G^\ddagger = +48.0 \text{ kcal mol}^{-1}$) to give the protonated cycloadduct **exo-11-H⁺**. In line with experimental results, the calculations (even though the barriers might be overestimated) clearly demonstrate that a simple Brønsted acid catalysis is not likely to be the origin of the high activities.

We next focused our attention on the potential Lewis acid catalysis by AlMe_3 as catalyst (Scheme 8). Again, the first step is the activation of the lactone through coordination to the Lewis acid. Based on our calculations this is a favourable process ($\Delta G = -11.3 \text{ kcal mol}^{-1}$) that should occur readily. Again, all identified transition state structures resulted in stepwise reactions as discussed for the Brønsted acid catalysis above. The formation of the first C–C bond proceeds with an activation free energy of $14.8 \text{ kcal mol}^{-1}$ through **TS3a** and results in the zwitterionic intermediate **(E)-13-AlMe₃**. Similar to the Brønsted acid catalysis described above, the formation of a Z-configured intermediate is also possible for AlMe_3 and proceeds with a comparable barrier. The zwitterion collapses in the next step without significant barrier via **TS3b** ($\Delta G^\ddagger = +1.5 \text{ kcal mol}^{-1}$) with only a very small barrier. Based on the computed activation free energy of $14.8 \text{ kcal mol}^{-1}$, a reaction should be observable in the presence of catalytic amounts of AlMe_3 , although no product formation was detected experimentally under the screening conditions. As other functionals (DSD-BLYP-D3BJ, $\omega\text{B97X-D}$, B3LYP-D3BJ) resulted in similar barriers around 15 kcal mol^{-1} , we can exclude a systematic error in the M06-2X calculations. Similarly, our

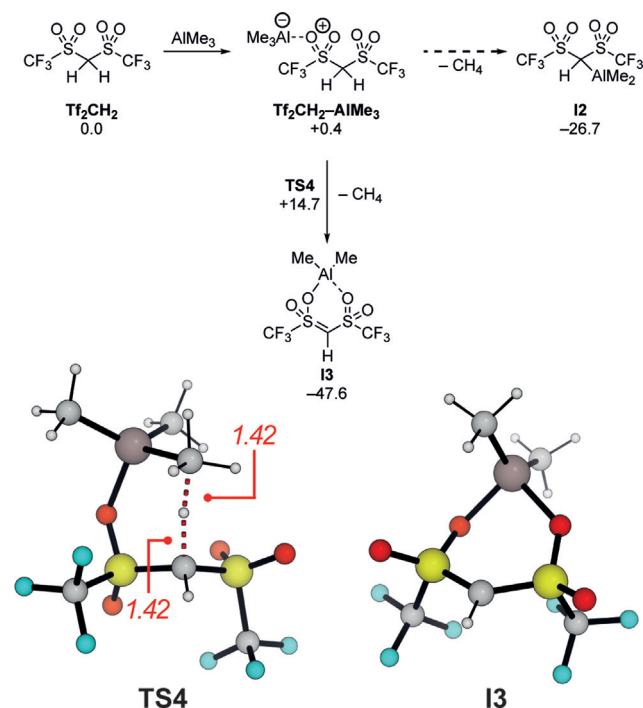


Scheme 8. Calculated Gibbs free energies (in kcal mol^{-1}) for the AlMe_3 -catalyzed cycloaddition between **7** and **8** (above) and structure as well as selected bond lengths (in \AA) for the transition states **TS3** (below).

calculations further indicate that the interaction between AlMe_3 and with the lactone ($\Delta G = -11.3 \text{ kcal mol}^{-1}$) is slightly stronger than an interaction with any of the three oxygen atoms of Brassard's diene ($-7.5 < \Delta G < -4.1 \text{ kcal mol}^{-1}$). Therefore, we have to conclude that either the solvent, which is present in a large excess, or the product interacts with the Lewis acid and lowers the reactivity and in turn increase the activation free energy.

Finally, we addressed the full catalytic system consisting of Tf_2CH_2 and AlMe_3 . In previous investigations, Taguchi and co-workers proposed that Tf_2CH_2 reacts with AlMe_3 to form the aluminum methide **12** and methane. **12** could then either react as a stronger Brønsted or Lewis acid to catalyze the Diels–Alder reaction.^[33] Based on our calculations (Scheme 9), a Lewis acid-base pair is formed first in a thermoneutral reaction. The proposed aluminum methide **12** could then be formed in an exergonic reaction ($\Delta G = -27.3 \text{ kcal mol}^{-1}$), but no transition states could be identified for this reaction. Instead, all transition states indicate that the isomeric O-substituted species **13** is formed instead. **13** is not only considerably more stable than its isomer **12**, but it is also formed through a small activation free energy of $14.4 \text{ kcal mol}^{-1}$ (**TS4**). The dual coordination of the AlMe_2 -fragment to both sulfonyl groups significantly contributes to the higher thermodynamic stability of **13**. The up-field shifts for the Tf_2CH -carbon and Tf_2CH -proton reported by Taguchi and co-workers are both in agreement with **12** and the isomeric structure **13**.

Both **12** and **13** could now act either as Brønsted acids or Lewis acids to catalyze the subsequent [4+2] cycloaddition.

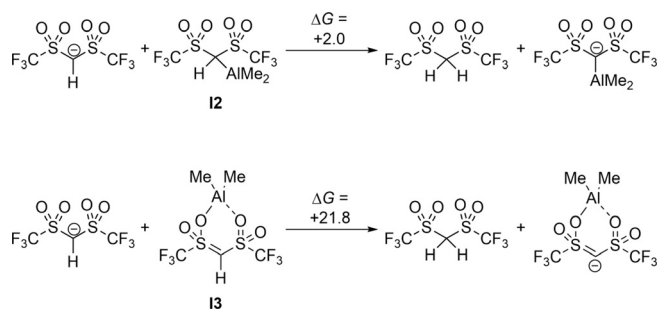


Scheme 9. Formation of the catalytically active species between Tf_2CH_2 and AlMe_3 (free energies in kcal mol^{-1}) (above) and structures of the transition state **TS4** and the potential catalyst **13** and selected bond lengths (in Å, below).

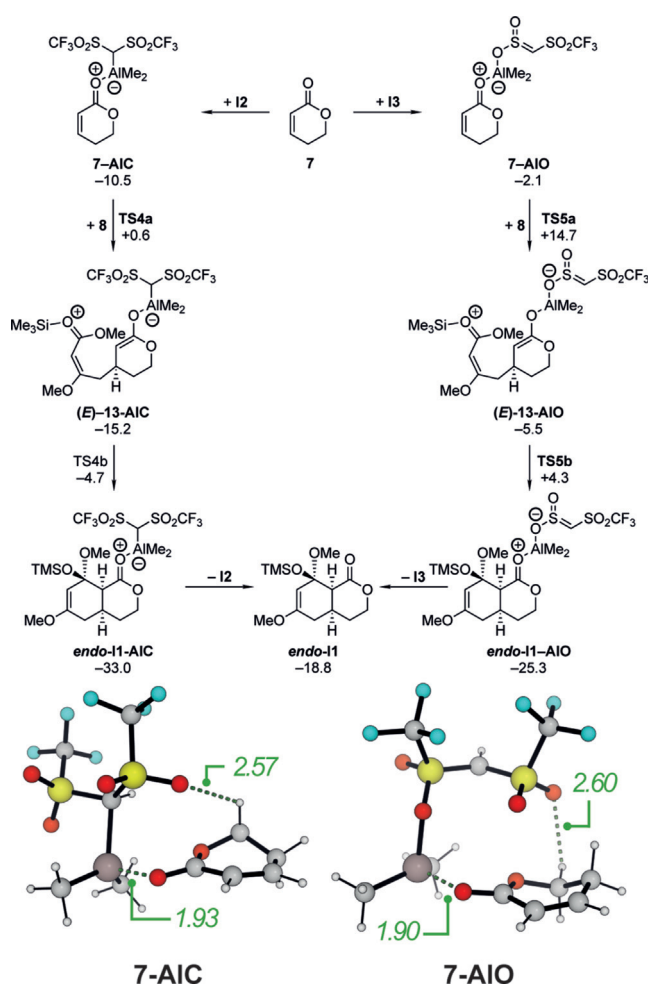
For an estimate of the change in Brønsted acidity, we calculated the reaction free energies for the isodesmic proton-transfer reactions as shown in Scheme 10. As these reactions are either almost thermoneutral (**12**) or highly unfavourable (**13**), one has to conclude that **12** and **13** cannot be considered as significantly stronger Brønsted acids compared to the free Tf_2CH_2 . Consequently, a Brønsted acid catalysis is rather unlikely as the origin of the catalytic activity.

Therefore, we focused on the Lewis acid catalysis pathway and wondered how **12** and **13** activate lactone **7**. The interaction of **12** with the lactone **7** leading to **7-AIC** is again an exergonic reaction and comparable yet slightly weaker than that of AlMe_3 (Scheme 11, left). Interestingly, the *Z*-configuration is more stable compared to the *E*-configuration, which might be attributed to the stronger C–H...O hydrogen bond (Scheme 11). However, the subsequent C–C bond formation occurs through **TS4a** with an activation free energy of only $11.1 \text{ kcal mol}^{-1}$. In contrast to the previous systems, the zwitterionic intermediate (**E**)-**13-AIC** next collapses through a comparable barrier of $10.5 \text{ kcal mol}^{-1}$ to give the *endo* cycloadduct **endo-11-AIC**. The higher stability of the zwitterionic intermediate with respect to the second bond formation also explains, why the Michael adduct **13** is observed as the main product in the absence of oxidants or fluoride salts (Scheme 1 d).

Alternatively, **13** could be the active catalyst of the AlMe_3 - Tf_2CH_2 mixture and the calculated Gibbs free energies are summarized in Scheme 11 (right). Based on our computations, the interaction of **13** with the lactone **7** is considerably weaker ($\Delta G = -2.1 \text{ kcal mol}^{-1}$) than that of **12**. In contrast, the direct comparison of the isomeric adducts **7-AIC** and **7-AIO** (Scheme 11, below) reveals, that the latter is thermodynamically preferred over the former by $12.4 \text{ kcal mol}^{-1}$ (not shown in Scheme 11). This can be attributed to the high intrinsic stability of the free Lewis acid **13**. Interestingly, no additional hydrogen bonds (e.g. between the $\text{Tf}_2\text{C-H}$ and the O-atom of the ester) stabilize these complexes. The subsequent C–C bond formation proceeds via **TS5a** with an activation barrier of $16.8 \text{ kcal mol}^{-1}$, followed by the cyclization via **TS5b** with an activation free energy of $9.8 \text{ kcal mol}^{-1}$. Again, the second C–C bond formation occurs much faster than the first one, but as the barriers of both steps are closer in energy than e.g. in Scheme 8, the life time of the intermediate (**E**)-**13-AIO** should also be larger.



Scheme 10. Calculated free energies for the isodesmic proton-transfer reactions between **12** and **13** and the Tf_2CH anion (in kcal mol^{-1}).



Scheme 11. Calculated Gibbs free energies (in kcal mol⁻¹) for the cycloaddition between **7** and **8** catalyzed by the Lewis acid **12** or **13** (above). Structure and selected bond lengths (in Å) for the complexes between **7** and **12** or **13**, respectively (below).

When comparing the different mechanistic pathways of Schemes 7, 8, 9, and 11, a Lewis acid catalysis by the AlMe₃-Tf₂CH₂-mixture results in the lowest activation free energy. Among the different isomers of the catalyst, the computational data indicate that **12** is most likely the catalytically active species. The calculated activation free energies for the Lewis acid catalyzed reactions are probably underestimated as both Lewis acids are likely to interact with the solvent molecules in the system. Given the similar interaction energies with carbonyl groups, it can be expected that the solvent-solute interactions are also comparable in both cases. These findings are also in line with previous ¹³C NMR investigations by Taguchi and colleagues, as a stronger change in chemical shifts was observed for AlMe₃-Tf₂CH₂ than for AlMe₃ alone.^[26] This indicates that coordination to the former results in a larger lowering of the LUMO of the Michael acceptor.

Conclusion

Experimental and computational investigations show that the reaction of 5,6-dihydro-2*H*-pyran-2-one (**7**) and (*Z*)-((1,3-dimethoxybuta-1,3-dien-1-yl)oxy)trimethylsilane (**8**) (Brasard's diene) catalyzed by AlMe₃ and Tf₂CH₂ undergoes a stepwise mechanism and no concerted *Diels-Alder* like reaction, making a competing vinylogous Michael addition possible. The experiments show that the major Michael-product is (*E*)-configured (**E**)-**13**, which could be verified by nOe-spectra and the convenient conversion into the cyclized product **12** by LHMDS. Oxidation of the intermediates **12** with DDQ gives the aromatic isocoumarins **14**. Overall, six mellein derivatives and four angelicin derivatives could be synthesized in moderate to good yields over three steps (30–84%). The computational results underline the experimental results, showing the vinylogous Michael addition and the AlMe₃/Tf₂CH₂-system as catalyst to be energetically favoured, in comparison to the direct formation of the *Diels-Alder* product and single AlMe₃ as catalyst.

Acknowledgements

We gratefully acknowledge the Studienstiftung des deutschen Volkes (Scholarship to A.W.), the Universität zu Köln, the Fonds der Chemischen Industrie, the Deutsche Forschungsgemeinschaft (GRK2158), the Heinrich-Heine-Universität Düsseldorf, the German Federal Ministry for Economic Affairs and Energy ("ZIM Kooperationsprojekt" KF3279X01AJ3), and the Forschungszentrum Jülich GmbH for their generous support of our project. We are grateful to the Regional Computing Center of the Universität zu Köln for providing computing time of the DFG-funded High-Performance Computing (HPC) System CHEOPS as well as for their support. We thank Birgit Henßen for analytic support. Open access funding enabled and organised by Projekt DEAL.

Conflict of interest

The authors declare no conflict of interest.

Keywords: catalysis · computational chemistry · density functional calculations · Michael additions · natural products

- [1] Y. Feng, X. Jiang, J. K. De Brabander, *J. Am. Chem. Soc.* **2012**, *134*, 17083–17093.
- [2] X. Huang, N. Shao, R. Huryk, A. Palani, R. Aslanian, C. Seidel-Dugan, *Org. Lett.* **2009**, *11*, 867–870.
- [3] X. Jiang, J. García-Fortanet, J. K. De Brabander, *J. Am. Chem. Soc.* **2005**, *127*, 11254–11255.
- [4] S. Wan, F. Wu, J. C. Rech, M. E. Green, R. Balachandran, W. S. Horne, B. W. Day, P. E. Floreancig, *J. Am. Chem. Soc.* **2011**, *133*, 16668–16679.
- [5] J. Yu, M. Yang, Y. Guo, T. Ye, *Org. Lett.* **2019**, *21*, 3670–3673.

- [6] M. Bielitzka, J. Pietruszka, *Angew. Chem. Int. Ed.* **2013**, *52*, 10960–10985; *Angew. Chem.* **2013**, *125*, 11164–11190.
- [7] R. H. Cichewicz, F. A. Valeriote, P. Crews, *Org. Lett.* **2004**, *6*, 1951–1954.
- [8] G. R. Pettit, J.-P. Xu, J.-C. Chapuis, R. K. Pettit, L. P. Tackett, D. L. Doubek, J. N. A. Hooper, J. M. Schmidt, *J. Med. Chem.* **2004**, *47*, 1149–1152.
- [9] Q. Liu, C. An, K. TenDyke, H. Cheng, Y. Y. Shen, A. T. Hoye, A. B. Smith, *J. Org. Chem.* **2016**, *81*, 1930–1942.
- [10] P. M. Scott, W. Van Walbeek, W. M. MacLean, *J. Antibiot.* **1971**, *24*, 747–755.
- [11] H. Zheng, C. Zhao, B. Fang, P. Jing, J. Yang, X. Xie, X. She, *J. Org. Chem.* **2012**, *77*, 5656–5663.
- [12] S. Khan, A. Sharma, H. Belrhali, M. Yogavel, A. Sharma, *J. Struct. Funct. Genomics* **2014**, *15*, 63–71.
- [13] W. A. Guiguemde, R. K. Guy, *Cell Host Microbe* **2012**, *11*, 555–557.
- [14] H. Nishikawa, *Bull. Agric. Chem. Soc. Jpn.* **1933**, *9*, 107–109.
- [15] C. Wohlfarth, T. Efferth, *Acta Pharm. Sin.* **2009**, *30*, 25–30.
- [16] K. Krohn, R. Bahramsari, U. Flörke, K. Ludewig, C. Kliche-Spory, A. Michel, H.-J. Aust, S. Draeger, B. Schulz, S. Antus, *Phytochemistry* **1997**, *45*, 313–320.
- [17] U. Höller, G. M. König, A. D. Wright, *J. Nat. Prod.* **1999**, *62*, 114–118.
- [18] F. Marinelli, U. Zanelli, V. N. Ronchi, *Phytochemistry* **1996**, *42*, 641–643.
- [19] M. Shibano, H. Naito, M. Taniguchi, N.-H. Wang, K. Baba, *Chem. Pharm. Bull.* **2006**, *54*, 717–718.
- [20] K. Anderson, F. Calo, T. Pfaffeneder, A. J. P. White, A. G. M. Barrett, *Org. Lett.* **2011**, *13*, 5748–5750.
- [21] H. Raistrick, C. E. Stickings, R. Thomas, *Biochem. J.* **1953**, *55*, 421–433.
- [22] D. Lai, A. Wang, Y. Cao, K. Zhou, Z. Mao, X. Dong, J. Tian, D. Xu, J. Dai, Y. Peng, L. Zhou, Y. Liu, *J. Nat. Prod.* **2016**, *79*, 2022–2031.
- [23] K. Koch, J. Podlech, E. Pfeiffer, M. Metzler, *J. Org. Chem.* **2005**, *70*, 3275–3276.
- [24] B. Verastegui-Omaña, D. Rebollar-Ramos, A. Pérez-Vásquez, A. L. Martínez, A. Madariaga-Mazón, L. Flores-Bocanegra, R. Mata, *J. Nat. Prod.* **2017**, *80*, 190–195.
- [25] Y. Zhang, Y. Tian, P. Xiang, N. Huang, J. Wang, J.-H. Xu, M. Zhang, *Org. Biomol. Chem.* **2016**, *14*, 9874–9882.
- [26] A. Saito, H. Yanai, T. Taguchi, *Tetrahedron Lett.* **2004**, *45*, 9439–9442.
- [27] T. Sambaiah, L.-P. Li, D.-J. Huang, C.-H. Lin, D. K. Rayabarapu, C.-H. Cheng, *J. Org. Chem.* **1999**, *64*, 3663–3670.
- [28] Z. Liu, X. Lin, N. Yang, Z. Su, C. Hu, P. Xiao, Y. He, Z. Song, *J. Am. Chem. Soc.* **2016**, *138*, 1877–1883.
- [29] K. C. Nicolaou, S. A. Snyder, T. Montagnon, G. Vassilikogiannakis, *Angew. Chem. Int. Ed.* **2002**, *41*, 1668–1698; *Angew. Chem.* **2002**, *114*, 1742–1773.
- [30] J.-A. Funel, S. Abele, *Angew. Chem. Int. Ed.* **2013**, *52*, 3822–3863; *Angew. Chem.* **2013**, *125*, 3912–3955.
- [31] J. Savard, P. Brassard, *Tetrahedron Lett.* **1979**, *20*, 4911–4914.
- [32] T. Ikeda, S. Yue, C. R. Hutchinson, *J. Org. Chem.* **1985**, *50*, 5193–5199.
- [33] H. Yanai, A. Takahashi, T. Taguchi, *Tetrahedron* **2007**, *63*, 12149–12159.
- [34] M. Tamiya, K. Ohmori, M. Kitamura, H. Kato, T. Arai, M. Oorui, K. Suzuki, *Chem. Eur. J.* **2007**, *13*, 9791–9823.
- [35] C. Kowalski, X. Creary, A. J. Rollin, M. C. Burke, *J. Org. Chem.* **1978**, *43*, 2601–2608.
- [36] M. W. Rathke, *J. Am. Chem. Soc.* **1970**, *92*, 3222–3223.
- [37] B. L. Lucht, D. B. Collum, *J. Am. Chem. Soc.* **1994**, *116*, 6009–6010.
- [38] T. Fischer, J. Pietruszka, *Adv. Synth. Catal.* **2012**, *354*, 2521–2530.
- [39] T. Fischer, J. Pietruszka, *Adv. Synth. Catal.* **2007**, *349*, 1533–1536.
- [40] D. Böse, P. Niesobski, M. Lübecke, J. Pietruszka, *J. Org. Chem.* **2014**, *79*, 4699–4703.
- [41] S. Bartlett, D. Böse, D. Ghori, B. Mechsner, J. Pietruszka, *Synthesis* **2013**, *45*, 1106–1114.
- [42] G. N. Vyas, N. M. Shah, *Org. Synth.* **1951**, *31*, 90.
- [43] S. Fiorito, F. Epifano, V. A. Taddeo, S. Genovese, *Tetrahedron Lett.* **2016**, *57*, 2939–2942.
- [44] See the Supporting Information for details of the employed computational methods.

Manuscript received: June 12, 2020

Accepted manuscript online: June 22, 2020

Version of record online: August 18, 2020